Effects of noise and variations on the duration of transient oscillations in unidirectionally coupled bistable ring networks

Yo Horikawa* and Hiroyuki Kitajima
Faculty of Engineering, Kagawa University, Takamatsu 761-0396, Japan
(Received 18 January 2009; revised manuscript received 2 June 2009; published 28 August 2009)

We study effects of spatiotemporal noise and spatial variations on long-lasting transient oscillations in ring networks of unidirectionally coupled bistable elements (neurons), the duration of which increases exponentially with the number of neurons. On the one hand, spatiotemporal noise tends to sustain the transient oscillations. The duration of the oscillations occurring from fixed initial conditions changes nonmonotonically with noise strength and takes the maximum value at intermediate noise strength. Further, the duration of the oscillations is distributed in the form of the second power law and the mean duration increases with the number of neurons in the presence of an optimal noise. On the other hand, spatial variations degrade the exponential increases in the duration of the oscillations with the number of neurons. In the presence of fixed biases in the steady states of the neurons, there is a flat region in the distribution of the duration of the oscillations occurring under random initial conditions and an increase in the mean duration is almost linear with the number of neurons. Further, the duration of the oscillations in an ensemble of the networks with random biases drawing from an identical distribution is distributed in the form of the second power law and the ensemble mean increases in proportion to the five-halves power of the number of neurons.

DOI: 10.1103/PhysRevE.80.021934 PACS number(s): 87.19.lj, 05.40.−a, 05.45.−a

I. INTRODUCTION

Nonlinear coupled dynamical systems, which show various spatiotemporal patterns, synchronization of oscillations, complicated bifurcations and chaos, have been of wide interest in various fields [1]. In this paper we consider ring networks of unidirectionally coupled elements with sigmoidal input-output relations. We call this network and the element a ring neural network and a neuron, respectively, according to the conventional use, though the structure of the network is rather simple and is not so related to artificial neural networks and actual nervous systems. The ring neural networks have been studied from the viewpoint of dynamics of neural networks [2], for recurrent neural networks [3], and as cyclic feedback systems [4]. Further, it has been shown that the discrete systems of them have multiple stable orbits [5], the networks with delays cause various spatiotemporal patterns [6] and long-lasting transient oscillations [7,8], and the networks with inertia show complicated and chaotic response [8]. These various properties are of general interest in nonlinear sciences apart from neural networks.

When the number of negative couplings is even and the coupling gains are larger than unity, the ring neural networks are globally bistable. Recently, however, it was shown that the networks without delays show long-lasting transient oscillations in computer simulation [9,10] and in experiments on its analog circuit [11]. Further, the duration of the transient oscillations was shown to increase exponentially with the number of neurons in the networks [12]. The networks then never reach their stable steady states in a practical time when the number of neurons is large. This exponential dependence of transient time on system size is of importance since it is difficult to distinguish transient states and asymptotically stable states, and to know which is observed then in actual systems. Although rings of a large number of elements are rather artificial, their properties are of interest from a viewpoint of the dynamics of nonlinear systems.

Exponential increases in transient time with system size were first found in transient patterns (kinks, fronts, and pulses) in a one-dimensional bistable reaction-diffusion equation, in which the motion of the patterns becomes extremely slow as the size of domains increases [13]. It has been shown that the duration of these transient patterns increases exponentially with the length of domains [13,14]. Similar extremely slow motion of patterns has been found in several high-dimensional reaction-diffusion systems, which are applied to combustion, chemical reaction, cell biology, nerve spike propagation, ecological systems, and population dynamics, for instance [15], and is called metastable dynamics or dynamic metastability [16]. Further, such exponential dependence has also been found in several complex systems, e.g., transient chaos in coupled map lattices, reaction-diffusion equations and networks of pulse-coupled neurons [17], and ordered patterns in neural networks [18].

The mechanism of the exponential increases in the duration of the oscillations in the ring neural networks was explained with a kinematical model of the traveling waves [12]. The oscillations are caused by the propagating boundaries and inconsistencies between the blocks of the neurons in which the signs of their states are the same. Similar traveling waves, the duration of which is expected to show exponential dependence on the number of elements, were also reported in a discrete time coupled system with elements of cubic nonlinearity [9]. This kinematics of the traveling waves in the networks is qualitatively the same as that of the metastable patterns in the reaction-diffusion systems [13–16]. The kinks and pulses interact with each other through their wave forms, the strength of which decreases exponentially with distances between them. Symmetric bistability and linear relaxation are common to these systems and

*Corresponding author. FAX: +81-87-864-2262; horikawa@eng.kagawa-u.ac.jp

are essential for the exponential increases in the transient time with the system size.

Similar kinematics also exists in spike propagation in a nerve fiber [19] and car-following models in traffic flow problems [20]. In a nerve spike train, it is known that the speeds of spikes depend on the interspike intervals to the preceding spikes owing the recovery process of nerve membrane. A finite spike train is then unstable but can sustain in a nerve fiber of actual length since difference in the speeds decreases exponentially with the interspike intervals. In a traffic flow, it has been shown that changes in patterns of traffic jams are very slow in a second-order optimal velocity model with delay [21]. The largest Floquet multiplier of unstable periodic solutions decreases to unity exponentially with the number of cars on a single-lane circular road, which implies the duration of the associated traffic jams increases exponentially with the number of cars. This property of the Floquet multiplier is also the same with that of the unstable periodic solution in the ring neural networks [10].

Further, the structure of the ring neural network is qualitatively the same as that of a ring oscillator, which is a circular chain of inverters and sometimes including buffers [22]. It generates stable oscillations when the number of inverters is odd and is widely used as an easy variable-frequency oscillator. Several dozens of inverters are used to obtain oscillations of low frequency for practical use and it is known that unfavorable oscillations of higher harmonics happen to be observed. Although such higher harmonics are considered to be unstable and transient unless inductance or inertia exists [23], they can be sustained in a long time owing to exponential increases in transient time with system size. Thus the properties of the ring neural networks are also of interest in the field of electronics engineering.

In actual networks and circuits, however, spatiotemporal fluctuations and variations are inevitable. It is known that they can cause various qualitative changes in behaviors in nonlinear systems, e.g., noise-induced phase transitions, oscillations and synchronization, stochastic and coherence resonances, and the generation and motion of spatiotemporal patterns [24]. Concerning to metastable transient patterns in the reaction-diffusion systems, it has been shown that spatial inhomogeneity stabilizes standing stationary patterns, which is known as pinning [25]. It has also been shown that asymmetry in the reaction function degrades the increasing rates of the duration of the transient fronts to a polynomial order of the domain size, while spatiotemporal noise tends to increase their duration [14]. In the ring neural networks, the same tendency to degradation in the increasing rates of the duration of the oscillations was reported in the experiment with an analog circuit and it was ascribed to random offset voltages in operational amplifiers [11,12]. It was also shown that spatiotemporal noise causes characteristic correlations in a series of the periods of oscillations in the networks of ring oscillator type [26,27].

In this study we consider effects of spatiotemporal fluctuations and spatial variations on the duration of the transient oscillations in the ring neural networks with a kinematical model of the traveling waves, in which noise and variations are taken into account. The high-dimensional differential equation system of the network with a large number of neurons is reduced to a first-order differential equation of the locations of the traveling waves with a fluctuation term. The kinematical approach makes difficulty due to the high-dimensionality tractable. The kinematics is common to exponential dependence of transient time on system size in coupled or extended symmetric bistable systems as well as the reaction-diffusion systems, so that it can be applied to transient patterns in them, e.g., traffic flow models and discrete time coupled systems. Further, the kinematical approach might be applicable to chaotic transient behaviors in the complicated systems, e.g., coupled map lattices and neural networks.

The rest of the paper is organized as follows. A model of the ring neural network with noise and variations is given in Sec. II. Transient behaviors of the networks are then shown with computer simulation. Effects of spatiotemporal noise in the duration of the transient oscillations are considered in Sec. III. It is then shown that the mean duration of the oscillations occurring from fixed initial conditions increases in the presence of noise of intermediate strength, which is a resonancelike behavior. Further, the distribution of the duration has the form of a power law of exponent 2 and the mean duration increases with the number of neurons. A part of the results in Sec. III was already reported in [26]. In Sec. IV, effects of random biases in the output functions of the neurons on the duration of the transient oscillations are considered. It is then shown that random biases degrade the exponential increases in the duration of the oscillations so that the duration increases almost linearly with the number of neurons. However, the duration of the oscillations occurring from fixed initial conditions can increase in the presence of random biases of intermediate variations. Further, the distribution of the duration occurring under random initial conditions has the form of a power law of exponent 2 in an ensemble of the networks with random biases under an identical distribution, and the mean duration in the ensemble increases with the five-halves power of the number of neurons. Finally, conclusion and future work are given in Sec. V. The properties of the duration of the transient oscillations in the absence of noise and variations are summarized in the Appendix for readers' sake.

II. RING NEURAL NETWORKS WITH NOISE AND RANDOM BIASES

The following ring networks of neurons are considered:

$$dx_1(t)/dt = -x_1(t) + f[x_L(t) - x_{b(L)}] + \sigma_x w_1(t),$$

$$dx_n(t)/dt = -x_n(t) + f[x_{n-1}(t) - x_{b(n-1)}] + \sigma_x w_n(t), \quad (2 \le n \le L),$$

$$f(x) = \tanh(gx), \quad (g > 1),$$

$$E\{w_n(t)\} = 0, \quad E\{w_n(t)w_{n'}(t')\} = \delta_{nn'}\delta(t-t'),$$

$$E\{x_{b(n)}\} = m_b, \quad E\{(x_{b(n)} - m_b)(x_{b(n')} - m_b)\} = \sigma_b^2 \delta_{nn'}, \quad (1)$$

where x_n is the state of the nth neuron, L is the number of neurons, $f(x)$ is the output function of the neurons, and g is

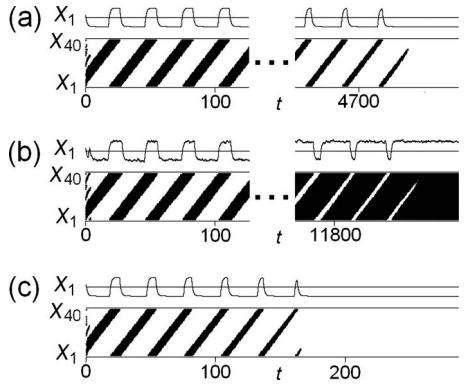

FIG. 1. Spatiotemporal patterns of the states of neurons in the network of $L=40$ and $g=10.0$ with no noise and biases (a), with noise ($\sigma_x=0.1$) (b), and with random biases ($m_b=0, \sigma_b=0.01$) (c). Upper panels: time series $x_1(t)$ of the state of the first neuron. Lower panels: the states of neurons (positive: black, negative: white).

the coupling gain. The neurons are unidirectionally coupled and the output of each neuron is transmitted to the next neuron successively. The output of the Lth neuron is then fed back into the first neuron. Gaussian white noise $w_n(t)$ with the strength σ_x is added to each neuron independently. The random bias $x_{b(n)}$ with the mean m_b and variance σ_b^2 in the output function is also added and is fixed randomly for each n $(1 \le n \le L)$.

In the absence of noise and biases, the origin $x_n=0$ $(1 \le n \le L)$ is globally stable when the absolute value of the coupling gain is less than 1 ($|g|<1$). When the couplings are positive and $g>1$, the network has a pair of the nonzero steady states: $(x_1, x_2, \ldots, x_L) = \pm(x_p, x_p, \ldots, x_p)$, $x_p = f(x_p)$ $(x_p > 0)$ and is globally bistable. It has been shown that it takes a long time for the network to reach one of the steady states when the number of neurons is large during which the states of the neurons oscillate [9–12]. Figure 1(a) shows an example of spatiotemporal patterns in the states of the neurons in the network with $g=10.0$ and $L=40$ under random initial conditions on $x_n(0)$. A time series $x_1(t)$ of the state of the first neuron is shown in the upper panel. A spatiotemporal pattern of the states of the neurons is shown in the lower panel, in which black and white regions correspond to the states of positive and negative sings, respectively. In the transient states, the neurons are divided in two blocks, in which the signs of their states x_n are the same in each block, i.e., positive or negative and between which the signs differ. Two boundaries of the two blocks then propagate in the direction of the couplings as $(x_1, x_2, \ldots, x_L)$:$(+,+,+,\cdots,+/,-,-,-,\cdots,-/) \rightarrow (-/,+,+,\cdots,+,+/,-,-,\cdots,-) \rightarrow (-,-/,+,\cdots,+,+,+/,-,\cdots,-) \rightarrow \cdots$, where slashes denote boundaries. The states of the neurons change their signs as the boundaries pass and then the network oscillates. This mechanism of the oscillations is quantitatively the same as a ring oscillator, which is a circular chain of inverters and shows stable oscillations [22].

The transient oscillations are such traveling waves of the boundaries of the blocks. The velocities of the boundaries depend exponentially on the numbers of neurons in the blocks (the block lengths) [12], which will be shown in Sec. III. As the number of neurons increases it can take an exponentially long time until the two blocks merge depending on the initial states, so that the network reaches one of the steady states and the oscillation ceases. Further the duration of the oscillations occurring from random initial states is distributed in a power-law form of exponent 1. The properties of the duration of the transient oscillations in the absence of noise and biases are shown in the Appendix. Note that, although we use the positive common coupling gain $g>1$ for simplicity, the networks with even numbers of neurons and negative coupling gains less than the value of the Hopf bifurcation point $[g<-1/\cos(\pi/L)]$ are equivalent to the networks of positive coupling gain through changes in the signs of the states of the alternate neurons $(x_{2m} \rightarrow -x_{2m}, 1 \le m \le L/2)$. Further, when the coupling gains vary in neurons, the network is equivalent to that with the all positive coupling gains through appropriate changes in the signs if the number of negative coupling gains is even. When the number of negative coupling gains is odd, however, the network qualitatively changes its property and can show a stable oscillation, which corresponds to a ring oscillator.

However, spatiotemporal noise and random biases have effects on the duration of the transient oscillations. Figure 1(b) shows a transient pattern in the states of the neurons in the network with noise of strength $\sigma_x=0.1$ under the same random initial condition as that in Fig. 1(a). It can be seen that the noise causes random fluctuations in the wave form of the state of the first neuron. Further, the duration of the oscillation last longer than that without noise (a) and the network reaches to another steady state $(x_n=x_p(1 \le n \le L))$. In Sec. III, it will be shown that the spatiotemporal noise tends to extend the duration of the transient oscillations. Figure 1(c) then shows a transient pattern in the states of the neurons in the network with random biases of mean $m_b=0$ and variance $\sigma_b^2=0.01^2$ under the same initial condition, in which it can be seen that the oscillation ceases quickly. In Sec. IV, it will be shown that the spatial biases degrade the increasing rate of the duration of the oscillations from an exponential order to a polynomial order of the number of neurons.

III. INCREASES IN THE DURATION OF THE OSCILLATIONS DUE TO SPATIOTEMPORAL NOISE

In this section, we consider effects of additive spatiotemporal noise $\sigma_x w_n(t)$ on the duration of the transient oscillations in the ring neural networks with the positive couplings with the gain larger than unity $(g>1)$. The random biases in Eq. (1) are set to be zero $(x_{b(n)}=0, 1 \le n \le L)$ in this section. As mentioned in Sec. II, the neurons are divided in blocks by the signs of their states and the boundaries of the blocks propagate in the network. The blocks merge with each other and finally two blocks remain as can be seen from Fig. 1. In the following, we derive a kinematical model of the traveling boundaries of two blocks of the neurons [26].

A. Kinematics of traveling waves with noise

Figure 2 shows a schematic diagram of changes in the states of $n-1$st and nth neurons (a) and a spatial pattern of

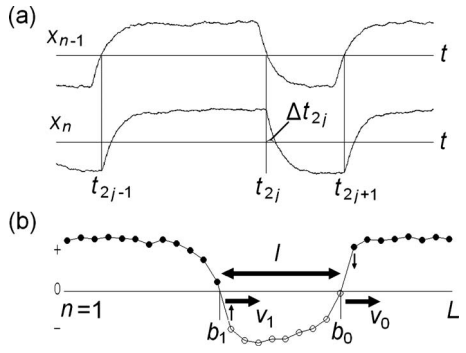

FIG. 2. Schematic diagram of changes in the states of $n-1$st and nth neurons (a) and a spatial pattern of the states of neurons (b).

the states of neurons (b) in the presence of spatiotemporal noise. Consider the state x_{n-1} of the $n-1$st neuron, and let t_{2j} be the time at which the state x_{n-1} changes from positive to negative and t_{2j+1} be the time at which the state x_{n-1} changes from negative to positive ($j \geq 0$) [Fig. 2(a)]. That is, the two boundaries in the network pass the $n-1$st neuron at t_{2j} and t_{2j+1} alternately. We here consider the boundary changing the signs of the states of the neurons from positive to negative. The other can be dealt with in the same manner. When the coupling gain g is large ($g \gg 1$), the output function $f(x)$ is approximated by the sign function (a step function),

$$\mathrm{sgn}(x) = -1, \quad (x \leq 0) = 1, \quad (x > 0). \tag{2}$$

In the absence of noise, the state of the nth neuron then changes in $t_{2j} \leq t < t_{2j+1}$ as follows [12]:

$$dx_n(t)/dt = -x_n(t) - 1, \quad (t_{2j} \leq t < t_{2j+1})$$

$$x_n(t) = \exp[-(t - t_{2j})][x_n(t_{2j}) + 1] - 1, \quad (t_{2j} \leq t < t_{2j+1}). \tag{3}$$

The propagation time Δt_{2j} of the boundary at the nth neuron is defined and obtained as

$$x_n(t_{2j} + \Delta t_{2j}) = 0,$$

$$\begin{aligned}\Delta t_{2j} &= \ln[1 + x_n(t_{2j})] \\ &= \ln\{1 + \exp[-(t_{2j} - t_{2j-1})][x_n(t_{2j-1}) - 1] + 1\} \\ &= \ln\{2 - 2\exp[-(t_{2j} - t_{2j-1})] + \exp[-(t_{2j} - t_{2j-2})] \\ &\quad \times [x_n(t_{2j-2}) + 1]\} \\ &\approx \ln 2 + \ln\{1 - \exp[-(t_{2j} - t_{2j-1})]\}.\end{aligned} \tag{4}$$

We neglect the second exponential term since its value is exponentially smaller than the first one. The propagation time of the boundary decreases as the interval to the forward boundary (the length of the forward block) decreases, and hence the propagation velocity increases.

The noise term $\sigma_x w_n(t)$ gives random variations in the propagation time. They are evaluated with the first passage time (FPT) t_p of the following equation:

$$dx_n(t)/dt = -x_n(t) - 1 + \sigma_x w_n(t),$$

$$x_n(0) \approx 1, \quad x_n(t_p) = 0, \tag{5}$$

where it is assumed that the numbers of neurons in the blocks are large and the neuron fully reaches the steady state $x_p = 1$ after the previous passage of the forward boundary. The mean $m(t_p)$ and variance $\sigma^2(t_p)$ of the FPT are expressed with the integral formulas [28] since Eq. (5) is equivalent to the Ornstein-Uhlenbeck (OU) process, but we here derive their approximate forms. When the variance of noise is small ($\sigma_x^2 \ll 1$), the mean of the FPT is approximated by $\Delta t = \ln 2$ in the absence of noise. The variance can be estimated with the probability density function of $x_n(t)$,

$$f[x_n(t)|x_n(0)] = 1/[(2\pi)^{1/2}\sigma_p]\exp\{-[x_n(t) - m_t]^2/(2\sigma_p^2)\},$$

$$m_t = [x_n(0) + 1]\exp(-t) - 1, \quad \sigma_p^2 = \sigma_x^2/2[1 - \exp(-2t)]. \tag{6}$$

The probability density function of the FPT is approximated by the Gaussian distribution with the same variance as Eq. (6) since the value of the slope of the trajectory at $x_n(t) = 0$ ($t = \ln 2$) in the absence of noise is minus unity ($d[2\exp(-t)]/dt|_{t=\ln 2} = -1$). Hence we obtain

$$\sigma^2(t_p) \approx 3/8 \cdot \sigma_x^2. \tag{7}$$

It can be shown that Eq. (7) agrees with the numerical integral of the formula for the OU process and the results of computer simulation of Eq. (5) for $\sigma_x < 0.1$. The propagation time of the boundary per neuron then becomes

$$\Delta t_{2j} \approx \ln 2 + \ln\{1 - \exp[-(t_{2j} - t_{2j-1})]\} + \sigma(t_p) w_j,$$

$$E\{w_j\} = 0, \quad E\{w_j w_{j'}\} = \delta_{jj'}. \tag{8}$$

Let b_0 and b_1 be the locations of the two boundaries ($0 \leq b_0, b_1 < L$) [Fig. 2(b)], and let l and $L-l$ be the lengths of the blocks with the neurons of negative and positive signs, respectively (the numbers of neurons in the two blocks), i.e.,

$$\begin{aligned} l &= b_0 - b_1, \quad (b_0 > b_1) \\ &= b_0 - b_1 + L, \quad (b_0 \leq b_1). \end{aligned} \tag{9}$$

The propagation velocity of the boundaries b_0 and b_1 is expressed by

$$\begin{aligned} v_0 &= db_0/dt \approx 1/\Delta t_{2j} \\ &= 1/(\ln 2 + \ln\{1 - \exp[-(t_{2j} - t_{2j-1})]\} + \sigma(t_p) w_{2j}), \end{aligned}$$

$$\begin{aligned} v_1 &= db_1/dt \approx 1/\Delta t_{2j+1} \\ &= 1/(\ln 2 + \ln\{1 - \exp[-(t_{2j+1} - t_{2j})]\} \\ &\quad + \sigma(t_p) w_{2j+1}). \end{aligned} \tag{10}$$

Finally we approximate the intervals $t_{2j} - t_{2j-1}$ and $t_{2j+1} - t_{2j}$ by $(L-l)\Delta t$ and $l\Delta t$ with $\Delta t = \ln 2$, respectively, since the difference in them only appear in double exponential terms. By subtracting the second equation from the first equation in Eq. (10), we then obtain the differential equation for changes in the block length l,

$$
\begin{aligned}
dl/dt &= db_0/dt - db_1/dt \\
&= 1/(\ln 2 + \ln\{1 - \exp[-\ln 2(L-l)]\} + \sigma(t_p)w_{2j}) \\
&\quad - 1/\{\ln 2 + \ln[1 - \exp(-\ln 2l)] + \sigma(t_p)w_{2j+1}\} \\
&\approx 1/(\ln 2)^2\{\exp[-\ln 2(L-l)] - \exp(-\ln 2l)\} + \sigma_l w(t) \\
&= k\{\exp[-c(L-l)] - \exp(-cl)\} + \sigma_l w(t),
\end{aligned}
$$

$$
k = 1/(\ln 2)^2, \quad c = \ln 2,
$$

$$
\sigma_l^2 = 2\sigma^2(t_p)/(\ln 2)^4 = 3/[4(\ln 2)^4]\sigma_x^2, \quad E\{w(t)\} = 0,
$$

$$
E\{w(t)w(t')\} = \delta(t-t'). \tag{11}
$$

The velocity of the boundary increases as the forward block length decreases and the two boundaries end up by colliding. The blocks merge and the oscillation then ceases. It has been shown that the duration T of the transient oscillations in the absence of noise increases exponentially with the number L of neurons [12]. The duration $T(l_0)$ of the oscillations with the initial block length $l(0)=l_0$ is given by Eqs. (A4) and (A5) as

$$
\begin{aligned}
T &= 1/(ck)\exp(cL/2)(\operatorname{arctanh}\{\exp[c(l_0 - L/2)]\} \\
&\quad - \operatorname{arctanh}[\exp(-cL/2)]) \approx [\exp(cl_0) - 1]\}/ck.
\end{aligned} \tag{12}
$$

B. Properties of the duration of the transient oscillations

In the presence of noise, the duration T of the transient oscillations is dealt with the FPT problem of the stochastic differential equation Eq. (10) with $l(T)=0$ or L. Following [28], the mean $m[T(l_0)]$ and variance $\sigma^2[T(l_0)]$ of the FPT beginning from the initial block length $l(0)=l_0$ are then obtained by

$$
m[T(l_0)] = 2\left\{\int_0^{l_0} \pi(\eta)d\eta \int_\eta^{L/2} [\sigma_l^2 \pi(\xi)]^{-1} d\xi\right\},
$$

$$
\begin{aligned}
\sigma^2[T(l_0)] &= 4\left\{\int_0^{l_0} \pi(\eta)d\eta \int_\eta^{L/2} m[T(\xi)]/[\sigma_l^2 \pi(\xi)]^{-1} d\xi\right\} \\
&\quad - m[T(l_0)]^2,
\end{aligned}
$$

$$
\pi(y) = \exp\left(-\int^y \frac{2a(\eta)}{\sigma_l^2} d\eta\right),
$$

$$
a(l) = k\{\exp[-c(L-l)] - \exp(-cl)\}, \tag{13}
$$

where we use a reflecting boundary at $l=L/2$ owing to the symmetry of the system since the expression is simpler than that with both absorbing boundaries at $l=0$ and L.

First, Fig. 3 shows the mean $m[T(l_0)]$ of the duration of the transient oscillations in the network with $L=40$ and $l_0=15$ against the noise strength σ_x. The mean duration of a thousand transient oscillations obtained with computer simulation of Eq. (1) with $g=10.0$ under the following initial condition is plotted with solid circles:

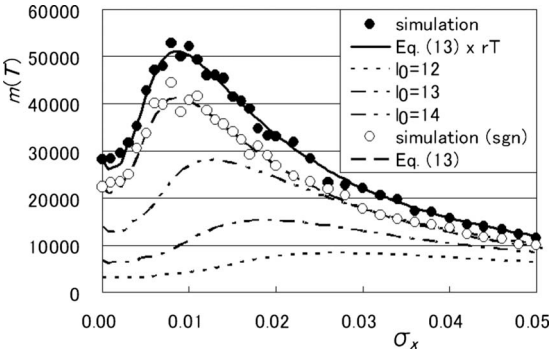

FIG. 3. Mean duration $m[T(l_0)]$ of the transient oscillations vs the noise strength σ_x in the network with $g=10.0$, $L=40$, and $l_0=15$. Numerical integral of Eq. (13) (a dashed line) multiplied by $r_T(=1.24)$ (a solid line), the mean duration of 1000 transient oscillations of computer simulation of Eq. (1) under the initial condition Eq. (14) with $g=10.0$ (solid circles) and with the sign function [Eq. (2)] (open circles). Plotted also are numerical integrals of Eq. (13) for $l_0=12$, 13, and 14 with dotted, dash-dotted, and dash-dot-dotted lines, respectively.

$$
\begin{aligned}
x_n(0) &= -1, \quad (1 \le n \le l_0) \\
&= 1, \quad (l_0 < n \le L).
\end{aligned} \tag{14}
$$

Equation (14) corresponds to the initial block length l_0 of the neurons of negative sign. The mean duration of those with the sign function Eq. (2) for $f(x)$ instead of $\tanh(gx)$ is also plotted with open circles. The mean duration changes nonmonotonically with the strength of noise and increases in the intermediate noise strength. This is never seen in the simple OU process and is a resonancelike phenomenon of interest; noise sustains the oscillations (noise-sustained oscillations). Numerical integral of Eq. (13) for the mean FPT is plotted with a solid line. The approximation by Eq. (13) agrees with the simulation results for the sign function (open circles). Note that the decreases in the mean FPT at small noise strength ($\sigma_x \approx 0.001$) may be an artifact due to the instability of the numerical integral since they do not appear in the simulation. In order to fit the mean FPT to the simulation results with the sigmoidal function $f(x)=\tanh(gx)$ in Eq. (1), we need to take account of the difference between the propagation time for the sigmoidal function and that for the sign function. The duration in the absence of noise obtained in the computer simulation is $T(l_0=15) \approx 28\,200$ [$f(x)=\tanh(gx), g=10.0$] and $T(l_0=15) \approx 22800$ [$f(x)$: sign function]. The mean FPT multiplied by this ratio $r_T \approx 1.24$ is plotted with a dashed line in Fig. 3 and it agrees with the simulation results (solid circles).

We just note a time step in computer simulation. Numerical calculation of Eq. (1) in the computer simulation was done using the simple Euler method with the time step 0.01 for the sigmoidal function. However, a smaller step is required in calculation when using the sign function [Eq. (2)] for f in Eq. (1). The unstable oscillations in this condition never cease with time steps larger than 10^{-5} in the absence of noise, which is a numerical artifact. In the presence of noise,

this artifact is relaxed and we take 0.001 for the time step. It was confirmed that about the same results are obtained by using smaller time steps.

Further, although we use the large value ($g=10.0$) for the coupling gains in this paper, it can be shown that the results of computer simulation with smaller coupling gains are qualitatively the same if the coupling gains are not so close to unity, e.g., $g \geq 1.2$. Exponential increases in the duration of the oscillations with the number of neurons in the networks for several values of g are shown in [10] and in Fig. 13 in the Appendix. The increasing rate of the logarithm of the duration of the oscillations approaches that in the networks with the sign function as the gain g increases.

When the number of neurons is large ($L \gg 1$), the FPT problem of simpler form is given by letting $\exp[-\ln 2(L-l)]$ be zero in Eq. (11) and $a(l)$ in Eq. (13) as

$$dl/dt = -k\exp(-cl) + \sigma_l w(t),$$

$$a(l) = -1/(\ln 2)^2 \exp(-\ln 2l). \tag{15}$$

It can be shown that the mean FPT calculated with Eq. (15) when $L=40$ agrees with the simulation results (data not shown). An intuitive explanation for the increase in the duration due to noise is as follows. The FPT of Eq. (15) in the absence of noise is given by $T(l_0)=\ln 2(2^{l_0}-1)$. The ratio of the increase $T(l_0+\Delta l)-T(l_0)$ due to a small positive fluctuation Δl in l_0 and the decrease $T(l_0)-T(l_0-\Delta l)$ due to a negative fluctuation $-\Delta l$ is $2^{\Delta l}$ and is always larger than 1. Then the fluctuations due to noise tend to increase the FPT. In the simple OU process, the deterministic term is linear and noise always decreases the FPT. The increases in the duration of the transient oscillations are due to the nonlinear exponential terms in Eq. (15).

Numerical integrals of Eq. (13) for $l_0=12$, 13, and 14 are also plotted with dotted, dash-dotted, and dash-dot-dotted lines, respectively, in Fig. 3. The peak of the mean duration moves toward the region of large noise strength and the maximum value decreases as the length l_0 of the initial block decreases. When starting with $l_0=L/2$, the oscillations never cease in the absence of noise since the velocities of the two boundaries are the same. The duration then monotonically decreases as the noise strength increases. When the initial states of the neurons are zero or randomly given about zero $[x_n(0)\approx 0]$, the mean duration of the transient oscillations is approximated by the integral of $T(l_0)/L$ over $0 \leq l_0 \leq L$ since the length of the initial block is considered to be uniformly distributed in $0 \leq l_0 \leq L$. The duration for the initial block length close to $L/2$ ($l_0 \approx L/2$) mainly contributes to it, and it can be shown that the mean duration monotonically decreases as the noise strength increases with computer simulation.

Next, we consider effects of the number of neurons for a fixed initial length l_0 of the block. Figure 4 shows the mean $m[T(l_0)]$ of the duration of the transient oscillations in the network, in which the initial length is fixed as $l_0=10$ and the number of neurons is changed as $L=40$, 60, 80, and 100. Plotted are numerical integrals of Eq. (13) multiplied by $r_T \approx 1.24$ (lines) and the mean duration of 10 000 transient oscillations obtained with computer simulation of Eq. (1) with

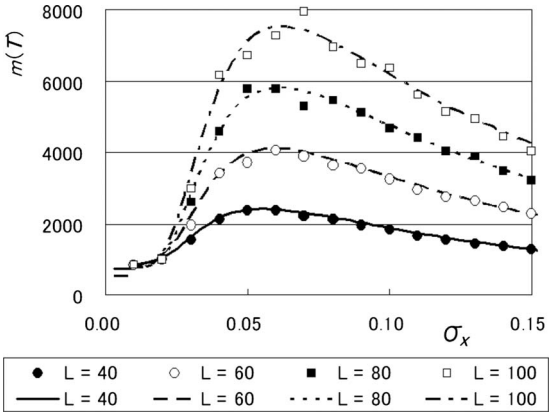

FIG. 4. Mean duration $m[T(l_0)]$ of the transient oscillations vs the noise strength σ_x in the networks with $l_0=10$ and $L=40$, 60, 80, and 100. Numerical integrals of Eq. (13) multiplied by $r_T(=1.24)$ (lines) and the mean duration of 10 000 transient oscillations of computer simulation of Eq. (1) with $g=10.0$ under the initial condition Eq. (14) (symbols).

$g=10.0$ under the initial condition Eq. (14) (symbols). The simulation results agree about with Eq. (13) though the variations are large when the number of neurons is large ($L=80, 100$). The peaks of the graphs of the mean duration slightly move toward the region of large noise strength as the number L of neurons increases. The maximum value increases in proportion to the length $L-l_0$ of the larger initial block. Note that the large variations in the sample means are due to a long tail in distribution of the duration shown below. In fact, the standard deviations of 10 000 data were several times as large as their means.

Further, Fig. 5 shows a normalized histogram of the duration of 20 000 transient oscillations obtained with computer simulation of Eq. (1) under Eq. (14) with $g=10.0$, $L=80$, and $l_0=10$ at the noise strength $\sigma_x=0.05$. The peak at $T \approx 500$ in the histogram corresponds to the duration of the oscillations in the absence of noise, in which the block length l decreases to zero so that $x_n(T)=1$ $(1 \leq n \leq L)$. The histogram then decreases in a power-law form and the exponent is about -2. The slope becomes gradual once at $T \approx 10^5$, which corresponds to the mean duration of the oscillations in which the block length reaches L so that $x_n(T)=-1$ $(1 \leq n \leq L)$.

The increase in the mean duration with the number $L-l_0$ of neurons in the larger initial block and the power-law distribution of the duration resemble those in the Wiener process with absorbing boundaries at $l=0$ and L, in which the mean FPT increases with the lengths between an initial position and the boundaries (l_0 and $L-l_0$) [28]. Further, the probability density function of the FPT is composed of those of the FPT to the two boundaries [$l(T)=0$ and L] and it has the form of $T^{-3/2}$ in the intermediate region, which is approximated by the inverse Gaussian distribution or the positive stable distribution with exponent 1/2 [29]. However, there is a difference in the exponent (-2 and $-3/2$) of the powers between the ring neural networks and the Wiener process.

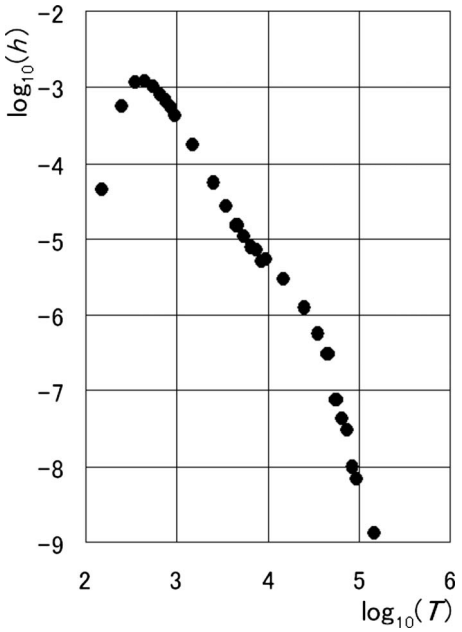

FIG. 5. Normalized histogram of the duration of 20 000 transient oscillations obtained with computer simulation of Eq. (1) under Eq. (14) with $g=10.0$, $L=80$, $l_0=10$, and the noise strength $\sigma_x=0.05$.

IV. DECREASE IN THE DURATION OF THE OSCILLATIONS DUE TO SPATIAL VARIATIONS

In this section, we consider effects of the random biases $x_{b(n)}$ on the duration of the transient oscillations in the ring neural networks. The strength of the spatiotemporal noise in Eq. (1) is set to be zero ($\sigma_x=0$) in this section. It has been shown that the exponential increases in the duration of the oscillations with the number of neurons [Eqs. (A4) and (A5)] are degraded in the results of the circuit experiment with operational amplifiers [11]. The decreases in the duration were then ascribed to random biases in the amplifiers with computer simulation [12]. In the following, properties of the duration of the transient oscillations in the presence of biases are derived with the kinematical model.

A. Kinematics of traveling waves with biases

First, we consider small common biases $x_{b(n)}=m_b$ ($1\leq n\leq L$) with $\sigma_b=0$. It is equivalent to shifts in the stable steady states by m_b when the output function is the sign function [Eq. (2)]. We use the following equation with a more general form of the output function:

$$dx_1/dt=-x_1+f_d(x_N),$$

$$dx_n(t)/dt=-x_n(t)+f_d[x_{n-1}(t)],\quad (2\leq n\leq L),$$

$$f_d(x)=-1+d_1,\quad (x\leq 0)$$

$$=1-d_2,\quad (x>0),\quad (|d_1|,|d_2|\ll 1). \tag{16}$$

The negative and positive steady states are shifted to the origin by d_1 and d_2, respectively. When $d_1=-d_2$, the shifts are equivalent to the common bias $m_b=d_1$. The propagation time Δt_j of the boundary between the blocks of the neurons in Eq. (16) then depends on the signs of the states of the neurons. The propagation time Δt_{2j} of the boundary changing the state of the nth neuron from positive to negative is approximated as

$$dx_n(t)/dt=-x_n(t)-1+d_1,\quad (t_{2j}<t\leq t_{2j+1}),$$

$$x_n(t)=\exp[-(t-t_{2j})][x_n(t_{2j})+1-d_1]-1+d_1,\quad (t_{2j}<t\leq t_{2j+1}),$$

$$\Delta t_{2j}=\ln[1+x_n(t_{2j})/(1-d_1)],\quad [x_n(t_{2j})>0,\ x_n(t_{2j}+\Delta t_{2j})=0],$$

$$\approx\ln[(2-d_1-d_2)/(1-d_1)]+\ln\{1-\exp[-(t_{2j}-t_{2j-1})]\},$$

$$x_n(t_{2j})\approx-(2-d_1-d_2)\exp(t_{2j}-t_{2j-1})+1-d_1, \tag{17}$$

where $x_n(t_{2j})$ is approximated by letting $x_n(t_{2j-1})=-1+d_1$. The propagation time Δt_{2j+1} of the boundary changing $x_n(t)$ from negative to positive is approximated in the same way as

$$dx_n(t)/dt=-x_n(t)+1-d_2,\quad (t_{2j+1}<t\leq t_{2j+2}),$$

$$x_n(t)=\exp[-(t-t_{2j+1})][x_n(t_{2j+1})-1+d_2]+1-d_2,\quad (t_{2j+1}<t\leq t_{2j+2}),$$

$$\Delta t_{2j+1}=\ln[1-x_n(t_{2j+1})/(1-d_2)],\quad [x_n(t_{2j+1})<0,\ x_n(t_{2j+1}+\Delta t_{2j+1})=0],$$

$$\approx\ln[(2-d_1-d_2)/(1-d_2)]+\ln\{1-\exp[-(t_{2j+1}-t_{2j})]\},$$

$$x_n(t_{2j+1})\approx(2-d_1-d_2)\exp[(t_{2j+1}-t_{2j})]-1+d_1. \tag{18}$$

Changes in the block length l (the number of neurons of negative sign) are approximated by

$$dl/dt\approx 1/\Delta t_{2j}-1/\Delta t_{2j+1}\approx 1/[\ln(2-d_1-d_2)]^2[\ln(1-d_1)-\ln(1-d_2)+\exp(-\Delta t(L-l))-\exp(-\Delta tl)]$$

$$\approx 1/(\ln 2)^2\{-d_1+d_2+\exp[-\ln 2(L-l)]-\exp(-\ln 2l)\},\quad (|d_1|,|d_2|\ll 1)$$

$$=kd+k\{\exp[-c(L-l)]-\exp(-cl)\},\quad [k=1/(\ln 2)^2,\ c=\ln 2,\ d=-d_1+d_2], \tag{19}$$

where we approximate as $t_{2j}-t_{2j-1}=(L-l)\Delta t$ and $t_{2j+1}-t_{2j}=l\Delta t$ with $\Delta t=\ln 2$. There is a small constant velocity kd ($d=-d_1+d_2$) owing to the shifts d_1 and d_2 in the steady states. The block length then tends to increase or decrease according to its sign. Intuitively, when the steady states are shifted to the origin, the attracting forces to them are weakened and the transient time to them increases. When the posi-

tive steady state is more shifted to the origin than the negative steady state ($d_2 > d_1$), the value of d is positive and the length l of the block with the neurons of negative sign increases so that the neurons in the network tend to reach the negative steady states ($-1+d_1$).

The common bias $x_{b(n)}=m_b$ is equivalent to the total shift $d=2m_b$ ($-d_1=d_2=m_b$). When biases vary randomly, the time in which the boundaries propagate around the network is just the sum of the propagation time of the all L neurons. Effects of random biases are thus approximated by those of the shifts in the steady states by letting the total shift be twice the mean of the biases, i.e. $d=2m(x_{b(n)})=2\Sigma_{n=1}^{L}x_{b(n)}/L$.

B. Duration of the oscillations with fixed initial block length

There are the following critical length l_c and total shift d_c in Eq. (19), below which the block length l decreases to zero, and over which l increases to L:

$$l_c = \ln\{2/[d + \sqrt{d^2 + 4\exp(-cL)}]\}/c,$$

$$d_c = \{\exp(-cl) - \exp[-c(L-l)]\}. \tag{20}$$

When d is positive ($d_2 > d_1$), the critical length l_c is smaller than $L/2$. The duration of the transient oscillations with the initial block length $l(0)=l_0$ is obtained as

$$T_1 = \ln[A(0)/A(l_0)]/[kc\sqrt{d^2 + 4\exp(-cL)}],$$
$$[l_0 < l_c,\ l(T_1) = 0],$$

$$T_2 = \ln[A(L)/A(l_0)]/\{kc\sqrt{[d^2 + 4\exp(-cL)}\ \},$$
$$[l_0 > l_c,\ l(T_2) = L],$$

$$A(l') = \frac{\exp(-cl') - [d + \sqrt{d^2 + 4\exp(-cl')}]}{\exp(-cl') - [d - \sqrt{d^2 + 4\exp(-cl')}]}, \tag{21}$$

where T_1 and T_2 correspond to the block length decreases to zero [$l(T_1)=0$] and increases to L [$l(T_2)=L$], respectively, so that the duration of the oscillations in which the states of the neurons reach $-1+d_1$ and $1-d_1$, respectively. Simpler forms of them for positive d are given by letting L be infinity in Eq. (19) as

$$dl/dt \approx k[d - \exp(-cl_+)],$$

$$l_c = \ln(1/d)/c, \quad d_c = \exp(-cl),$$

$$T_1 = \ln\{(1-d)/[1 - d\exp(cl_0)]\}/(ckd),$$
$$[l_0 < l_c,\ l(T_1) = 0],$$

$$T_2' = \ln\{[d\exp(cL) - 1]/[d\exp(cl_0) - 1]\}/(ckd),$$
$$[l_0 > l_c,\ l(T_2') = L],$$

$$T_2 = \ln(\{1 + d\exp[c(L-l_0)]\}/(1+d))/(ckd),$$
$$[l_0 > l_c,\ l(T_2) = L], \tag{22}$$

where T_2 is obtained by letting $d \to -d$, $l_0 \to L - l_0$, and $l(T_2)=0$, which gives better approximation of Eq. (21).

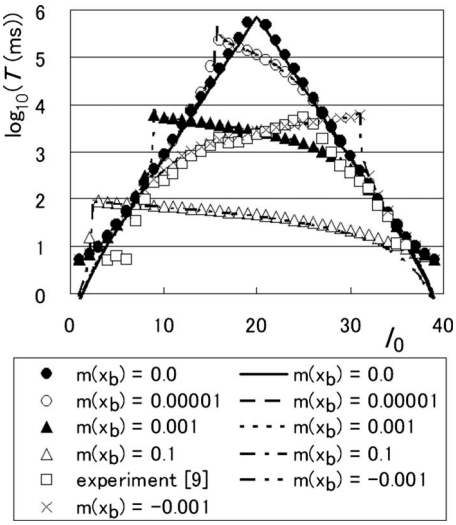

FIG. 6. Duration T of the transient oscillations vs the initial block length l_0 ($0<l_0<L$) with $L=40$ and $g=10.0$ in the presence of random biases of $\sigma_b=0.01$ and the mean $m(x_{b(n)})=0$, 10^{-5}, 10^{-3}, 10^{-1}. Plotted are examples of the results of computer simulation of Eq. (1) under Eq. (14) (symbols), Eq. (21) (lines), and Eq. (A4) for $m(x_{b(n)})=0$. The result of the experiment in [9] (open squares) and the result of simulation (crosses) and Eq. (21) with $m(x_{b(n)})=-10^{-3}$ (a dash-dot-dotted line) are also plotted.

For a fixed small total shift $d>0$, the duration T_1 increases exponentially with l_0 when $l_0<l_c$ and becomes infinity at $l_0=l_c$. Then T_2 decreases almost linearly with l_0 when $l_0>l_c$ as

$$T_1 \approx [\exp(cl_0) - 1]/(ck), \quad (0 < l_0 < l_c),$$
$$\to \infty, \quad (l_0 \to l_c),$$
$$T_2 \approx (L - l_0)/(kd), \quad (l_c < l_0 < L - l_c),$$
$$\approx \{\exp[c(L-l_0)] - 1\}/(ck), \quad (L - l_c < l_0 < L),$$
$$l_c \approx \ln(1/d)/c. \tag{23}$$

The duration increases exponentially with l_0 up only to $T_L = T_1(l_c) \approx (1-d)/(ckd)$ in the side regions $0<l_0<l_c$ and $L-l_c<l_0<L$. The increase in the duration is almost linear with l_0 in the middle region $l_c<l_0<L-l_c$ and is up to $T_{H1} = T_2(l_c) \approx (L-l_c)/(kd)$. The width of the region about $l_0 \approx l_c$ in which the duration increases over T_{H1} is exponentially small.

Figure 6 shows the duration T of the transient oscillations against the initial block length l_0 ($0<l_0<L$) with $L=40$ in the presence of random biases. The mean $m(x_{b(n)})(=d/2)$ of the biases is set to be 0, 10^{-5}, 10^{-3}, 10^{-1}. Plotted are examples of the results of computer simulation of Eq. (1) with $g=10.0$ under Eq. (14) (symbols), Eq. (21) for $m(x_{b(n)}) = 10^{-5}$, 10^{-3}, 10^{-1}, and Eq. (A4) for $m(x_{b(n)})=0$ (lines). In the simulation the values of the biases are drawn from Gaussian random numbers of the variance $\sigma_b^2=0.01^2$ and the mean $m(x_{b(n)})$ of the biases is adjusted by shifts. The duration in the simulation with the mean bias zero (solid circles) hardly changes from that [Eq. (A4)] in the absence of biases (a solid line) even though there are variations in the biases. As the

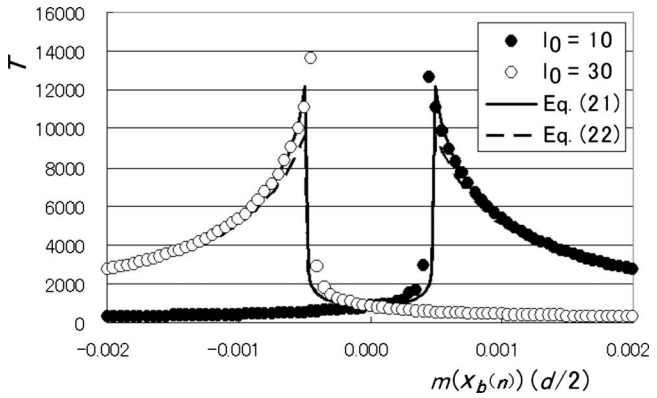

FIG. 7. Duration T of the transient oscillations vs the mean bias $m(x_{b(n)})$ for the initial block length $l_0=10$ and 30 with $L=40$. Plotted are examples of the results of computer simulation of Eq. (1) with $g=10.0$ under Eq. (14) (open and solid circles), Eq. (21) (a solid line), and Eq. (22) (a dashed line).

mean bias increases, the exponential increases in the duration degrade in the middle region ($l_0 \approx L/2$) and they only appear near the both sides ($l_0 \approx 0, L$). Equation (21) agrees with the simulation results for $m(x_{b(n)})=10^{-5}$, 10^{-3}, 10^{-1}. It can be shown that Eq. (22) also agrees with them except for $l_0 \approx l_c$ in T_2. It can also be shown that Eq. (23) agrees about with them though it is slightly smaller than them in the middle region ($l_c < l_0 < L-l_c$) (data not shown). Further, the result of the experiment in [11,12] is plotted with open squares. The result of the simulation (crosses) and Eq. (21) with $m(x_{b(n)}) = -10^{-3}$ (a dash-dot-dotted line) agree with it except for $l_0 \approx l_c$ ($l_c \approx 31.0$). The expected value of the standard deviation (SD) σ_b of the population of the biases is $m(x_{b(n)})L^{1/2} \approx 0.003$ and corresponds to 36 mV in the actual circuit. It is not so larger than the standard value of the OP amp (less than 10 mV). Note that it was checked with computer simulation that the duration hardly vary when the mean biases $m(x_{b(n)})$ are set to be the same even though the values of the biases vary randomly. It was also checked that the common biases by $m_b=m(x_{b(n)})$ in Eq. (1) and the shifts in the steady states by $d=2m(x_{b(n)})$ in Eq. (16) give almost the same results.

For a fixed initial length $l_0 < L/2$, the duration T_1 increases monotonically with d and becomes infinity at $d=d_c$. Then T_2 decreases in proportion to the inverse of d. Figure 7 shows the duration T of the transient oscillations against the mean bias $m(x_{b(n)})$ for the initial length $l_0=10$ and 30 with $L=40$. Plotted are examples of the results of computer simulation of Eq. (1) with $g=10.0$ under Eq. (14) (open and solid circles), Eq. (21) (a solid line), and Eq. (22) (a dashed line). Equations (21) and (22) agree with the simulation results though the location of the critical shift ($d_c \approx 0.000\,49$) slightly deviates. This is ascribed to the finite gain g and it can be shown the results of computer simulation with the sign function [Eq. (16)] are well fitted to Eqs. (21) and (22). Asymmetry or random biases in the steady states can then sustain the transient oscillations about the critical length and shift.

C. Duration of the oscillations under random initial conditions

When the initial states $x_n(0)$ of the neurons are given randomly about the mean m_b of the biases, the initial block lengths l_0 are regarded to be distributed uniformly in $(0,L)$. Using Eq. (21), the probability density function $h(T)$ of the duration T of the transient oscillations is then given by

$$h(T) = \left(\frac{1}{|dT_1/dl_0|} + \frac{1}{|dT_2/dl_0|} \right) / L$$

$$= \frac{ckDB_1 \exp(-ck\sqrt{DT})}{[y_2 - y_1 B_1 \exp(-ck\sqrt{DT})][1 - B_1 \exp(-ck\sqrt{DT})]}$$

$$+ \frac{ckDB_2 \exp(-ck\sqrt{DT})}{[y_2 - y_1 B_2 \exp(-ck\sqrt{DT})][1 - B_2 \exp(-ck\sqrt{DT})]},$$

$$d = 2m(x_{b(n)}), \quad D = d^2 + 4\exp(-cL),$$

$$y_1 = (d-D)/2, \quad y_2 = (d+D)/2,$$

$$B_1 = (1-y_2)/(1-y_1), \quad B_2 = [\exp(-cL) - y_2]/[\exp(-cL) - y_1]. \tag{24}$$

Using Eq. (22), it is given by

$$h(T) = \frac{kd}{L}\left[\frac{1-d}{\exp(ckdT) - 1 + d} + \frac{1+d}{-\exp(-ckdT) + 1 + d} \right], \quad (0 \le T \le T_U),$$

$$T_U = T_2(l_0 = l_c) = \frac{\ln(\{1 + d\exp[c(L-l_c)]\}/(1+d))}{ckd},$$

$$\{T_U \to [\exp(cL/2) - 1]/(ck), \quad (d \to 0)\}, \tag{25}$$

where the second term in the right-hand side of the first equation must be limited to T_U owing to the derivation of T_2 in Eq. (22). This upper bound T_U is equal to the maximum value $T(L/2)=[\exp(cL/2)-1]/(ck)$ in Eq. (A5) as well as the cutoff $T_c=\exp(cL/2)/ck$ in the absence of biases, below which the duration is distributed in the form of $1/T$ (the Appendix). Further, using Eq. (23), it is approximated as

$$h(T) \propto 1/T, \quad [T < T_L \approx (1-d)/(ckd)],$$

$$\approx \frac{L - 2l_c}{L(T_{H1} - T_{H2})} \approx kd/L, \quad [T_{H2} \approx l_c/(kd) = -\ln(d)/(ckd) < T < T_{H1}],$$

$$\propto \exp(-\lambda T), \quad (T > T_{H1} \approx (L - l_c)/(kd) = [L + \ln(d)/c]/(kd). \tag{26}$$

The power-law distribution for small T ($<T_L$) and the exponential distribution for large T ($>T_{H1}$) are the same properties as those in the absence of biases ($d=0$). However, the duration is uniformly distributed in the middle region $T_{H2} < T < T_{H1}$ of width $O(L/d)$ owing to the biases. This flat region corresponds to the linear increase of T_2 with l_0 in $(l_c, L-l_c)$ in Eq. (23). Further, the upper bound T_{H1} of the region increases only linearly with the number L of neurons

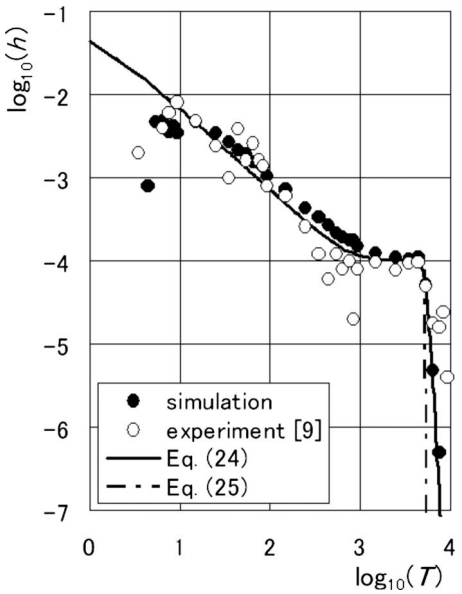

FIG. 8. Normalized histograms of the duration of 10 000 transient oscillations obtained with computer simulation of Eq. (1) with $g=10.0$, $L=40$, and $m(x_{b(n)})=0.001$ (solid circles) and of 500 transient oscillations observed in the experiment in [9] (open circles), Eq. (24) (a solid line) and Eq. (25) (a dashed line).

and not exponentially. Figure 8 shows normalized histograms of the duration of 10 000 transient oscillations obtained with computer simulation of Eq. (1) with $g=10.0$, $L=40$ and $m(x_{b(n)})=0.001$ (solid circles) and of 500 transient oscillations observed in the experiment in [11] (open circles). In the simulation, the values of the biases are drawn from Gaussian random numbers with $\sigma_b=0.01$ and the means adjusted to $m(x_{b(n)})=0.001$ by shifts, and the initial states $x_n(0)$ of neurons are drawn from Gaussian random numbers with the mean 0 and SD 0.1. Plotted also are the probability density functions of Eq. (24) (a solid line) and Eq. (25) (a dashed line). They hardly differ from each other except for $T\approx T_U$ ($\approx$5300) and agree with the simulation results. The values of T_L, T_{H1}, and T_{H2} in Eq. (26) are about 346, 2153, and 7455, respectively, which also agree about with the results of the simulation and experiment.

The mean duration $m(T)$ of the oscillations is evaluated with T_1 and T_2 in Eq. (23) as

$$m(T)=\left(\int_0^{lc} T_1 dl+\int_{l_c}^{L} T_2 dl\right)/L=\frac{L-2l_c}{2kd}+\frac{2(1/d-1+\ln d)}{c^2kL}$$
$$\approx\frac{L+2\ln(d)/c}{2kd}+\frac{2}{c^2kdL}. \quad (27)$$

The first term in the right-hand side corresponds to T_2 in $(l_c, L-l_c)$ and is dominant except for $d\to 0$, which is also derived with $h(T)$ in (T_{H2}, T_{H1}) in Eq. (26). The mean duration decreases in inversely proportion with the shift d $[=m(x_{b(n)})/2]$ and in proportion to the number L of neurons. The exponential increases in the duration of the transient oscillations with the number of neurons are then degraded in the presence of shifts or biases in the steady states.

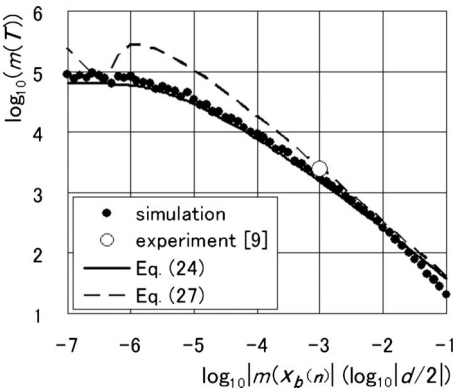

FIG. 9. Mean $m(T)$ of the duration of the transient oscillations vs the mean bias $m(x_{b(n)})$ $(=d/2)$ in the network of $L=40$ neurons. Plotted are the mean duration of 1000 oscillations obtained with computer simulation of Eq. (1) with $g=10.0$ for each bias (solid circles) and of 500 oscillations observed in the experiment in [9] (an open circle at $|m(x_{b(n)})|=0.001$), the numerical integral with Eq. (24) (a solid line), and Eq. (27) (a dashed line).

Figure 9 shows the mean $m(T)$ of the duration of the transient oscillations against the mean bias $m(x_{b(n)})$ $(=d/2)$ in the network of $L=40$ neurons. Plotted are the mean duration of 1000 oscillations obtained with computer simulation of Eq. (1) with $g=10.0$ for each bias (solid circles) and of 500 oscillations observed in the experiment in [11] [an open circle at $|m(x_{b(n)})|=0.001$]. Plotted also are the numerical integral $\int_0^\infty h(T)dT$ with Eq. (24) (a solid line) and Eq. (27) (a dashed line). In the simulation, the values of the biases are Gaussian random with $\sigma_b=0.01$ and the mean $m(x_{b(n)})$ adjusted in each, and the initial states $x_n(0)$ of neurons are Gaussian random with the mean $m(x_{b(n)})$ and SD 0.1. The estimates with Eq. (24) agree with the results of the simulation and experiment. It can be shown that the estimates with numerical integrals with Eqs. (25), (21), and (22) agree with them. Equation (27) gives rough estimates for the mean duration in the range $(T>10^{-7})$ in Fig. 9.

Figure 10 shows the mean duration $m(T)$ of the transient oscillations against the number L of neurons for a fixed mean bias $m(x_{b(n)})=0.01$. Plotted are the mean duration of 10 000 oscillations obtained with computer simulation of Eq. (1) with $g=10.0$ and random biases Gaussian with $\sigma_b=0.01$ and $m(x_{b(n)})=0.01$ under random initial conditions $x_n(0)$ of Gaussian with the mean 0 and SD 0.1 (solid circles). Plotted also are the estimates with the numerical integrals $\int_0^\infty h(T)dT$ with Eq. (24) (a solid line) and Eq. (25) (a dashed line), and Eq. (27) (a dotted line). [The numerical calculation with Eq. (24) in our system gives no results for $L\geq 70$ owing to numerical complexity.] The estimates with Eqs. (24) and (25) increase linearly with the number of neurons. Equation (27) is slightly larger than the estimates with Eqs. (24) and (25), but the increasing rates are almost the same. However, the increasing rate of the simulation results decreases as L increases $(L\geq 60)$ although they increase in proportion to L and agree with the estimates for $L\leq 50$. This decrease in the increasing rate is explained as follows.

It can be shown with computer simulation that the neurons are divided into four or more blocks, in which the signs

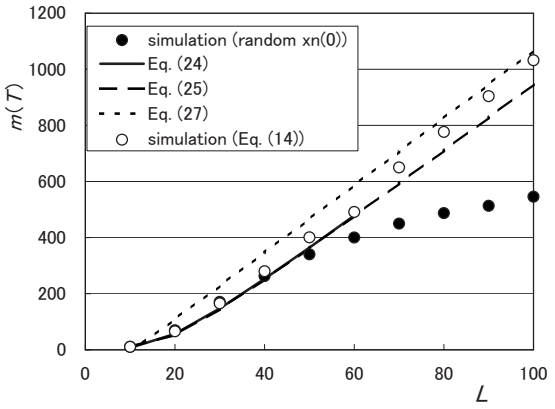

FIG. 10. Mean duration $m(T)$ of the transient oscillations vs the number L of neurons for a fixed mean bias $m(x_{b(n)})=0.01$. Plotted are the mean duration of 10 000 oscillations obtained with computer simulation of Eq. (1) with $g=10.0$ and random biases of σ_b 0.01 under random initial conditions $x_n(0)$ of mean 0 and SD 0.1 (solid circles), the numerical integrals with Eq. (24) (a solid line) and Eq. (25) (a dashed line), and Eq. (27) (a dotted line). Plotted also is the mean of the duration obtained with computer simulation of Eq. (1) under Eq. (14) for the initial length $l_0=1$ to L (open circles).

of the states are the same in each block, when the number of neurons is large, i.e. several blocks are generated. The blocks then merge one by one according to the same mechanism as that for two blocks, and finally two blocks remain. In this process the lengths l_0 of the negative blocks over and close to l_c, which result in long duration, increase in the presence of positive mean biases. Then the distribution of the length of the negative block in the final two blocks is not uniform in $(0,L)$ but is negatively skewed to L. The mean duration decreases consequently since the proportion close to zero is large. The same deviation occurs when the mean bias is negative. In fact, the mean $\Sigma_{l_0=1}^{L} T(l_0)/L$ of the duration obtained with computer simulation of Eq. (1) under Eq. (14) for the initial length $l_0=1$ to L is also plotted with open circles in Fig. 10, which approximates the mean duration under the uniform distribution of l_0 in $(0,L)$. It increases linearly even for large L as the estimates with Eq. (25), while the increasing rate is slightly larger.

D. Ensemble mean of the duration of the oscillations under an identical distribution of biases

Finally, we consider an ensemble of the networks consisting of the neurons the biases $x_{b(n)}$ of which obey the Gaussian distribution with the mean $m_b=0$ and SD σ_b. The mean of the biases $m(x_{b(n)})$ in each network then varies and obeys the Gaussian distribution with the mean 0 and SD $\sigma_b/L^{1/2}$, where L is the number of neurons in the network. The probability density function $h(T;\sigma_b)$ of the duration T of the transient oscillations occurring from random initial states $x_n(0)$ over an ensemble of the networks is then given by the following convolution:

$$h(T;\sigma_b) = \int h(T)h(d;\sigma_b)dd$$

$$= 2\int_0^{d_U} \frac{h(T)}{\sqrt{2\pi}\sigma_d}\exp[-d^2/(2\sigma_d^2)]dd,$$

$$d = 2m(x_{b(n)}), \quad \sigma_d = 2\sigma_b/L^{1/2},$$

$$d_U{:}T = \frac{\ln(\{1+d_U\exp[c(L-l_c)]\}/(1+d_U))}{ckd_U}, \tag{28}$$

where d_U comes from T_U in Eq. (25) and is used an appropriate upper bound for d. By replacing $h(T)$ with $m(T)$, an explicit form of $h(T;\sigma_b)$ is obtained as

$$h[m(T);\sigma_b] \approx h(d;\sigma_b)d\,d/dm(T)$$

$$\approx \frac{L}{2\sqrt{2\pi}\sigma_d km^2(T)}\exp\{-[L/2km(T)]^2/(2\sigma_d^2)\}$$

$$\approx \frac{L^{3/2}}{4\sqrt{2\pi}\sigma_b km^2(T)}\exp\left(\frac{-L^3}{32\sigma_b^2k^2m^2(T)}\right),$$

$$m(T) \approx \frac{L+2\ln(d)/c}{2kd} \approx L/(2kd),$$

$$d_L = \exp(-cL/2),$$

$$\left\{0 < m(T) < T_{H1}(d_L)[=T_{H2}(d_L)] = \frac{L\exp(cL/2)}{2k}\right\}, \tag{29}$$

where we use the first term $\{[L+2\ln(d)/c]/(2kd)\}$ in Eq. (27) for $m(T)$, and d_L comes from $m(T)=0$, which gives the upper bound $T_{H1}(d_L)$ for T. The distribution of the duration thus has a power-law form (T^{-2}) of exponent 2 for large T up to $T_{H1}(d_L)$. Figure 11 shows a normalized histogram of the duration of 10 000 transient oscillations obtained with computer simulation of Eq. (1) with $g=10.0$ and $L=40$ (solid circles). The biases $x_{b(n)}$ are drawn from the Gaussian distribution with $m_b=0$ and $\sigma_b=0.01$, and $x_n(0)$ are Gaussian random with the mean 0 and SD 0.1 in each run. Plotted also are the numerical integrals $h(T;\sigma_b)$ of Eq. (28) with Eqs. (24) and (25) for $h(T)$ with solid and dashed lines, respectively. They hardly differ from each other except $T\approx 10^6$ and agree with the simulation result. The slope of the graph is -1 for small T ($<10^3$), which might reflect the form of $1/T$ in $h(T)$ for $T<T_L$ in Eq. (26). The slope becomes once gradual and then steeper than -2 as T increases. Equation (29) is plotted with a dotted line, the slope of which is -2 for large T. The difference in the exponent of the power laws between the simulation result and Eq. (29) is ascribed to the upper bound T_U in Eq. (25) and the cutoff T_c ($\approx 7\times 10^5$ for $L=40$), beyond which the duration obeys the exponential distribution. This power-law form T^{-2} in the distribution appears clearly as the number L of neurons increases. A normalized histogram of the duration of 10 000 oscillations obtained with simulation (open circles) and Eq. (29) (a dash-dotted line) for $L=80$ are also plotted in Fig. 11. Equation (29) agrees with the simulation result for $T>10^4$ ($T_U\approx 10^{12}$).

The mean duration of the transient oscillations over an ensemble of the networks with random biases with the mean $m_b=0$ and SD σ_b is approximated using $m(T)$ and d_L in Eq. (29) as

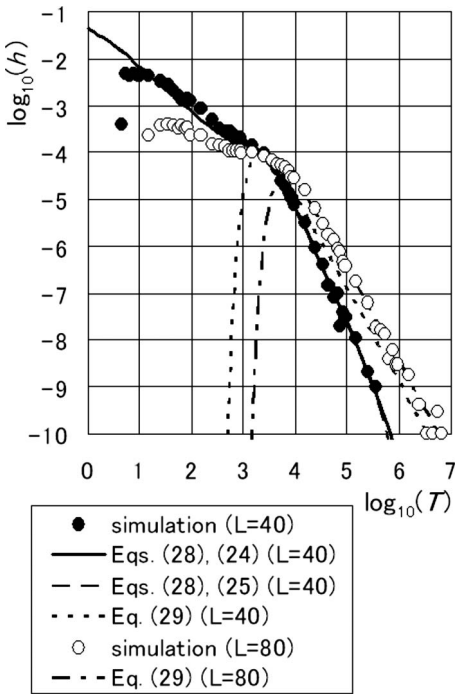

FIG. 11. Normalized histogram of the duration of 10 000 transient oscillations obtained with computer simulation of Eq. (1) with $g=10.0$, $L=40$, biases $x_{b(n)}$ of m_b 0 and σ_b 0.01 and the initial states $x_n(0)$ of neurons of the mean 0 and SD 0.1 (solid circles), the numerical integrals $h(T;\sigma_b)$ of Eq. (28) with Eq. (24) (a solid line) and Eq. (25) (a dashed line) for $h(T)$, and Eq. (29) (a dotted line). Plotted also are a normalized histogram of the duration of 10 000 oscillations obtained with simulation (open circles) and Eq. (29) (a dash-dotted line) for $L=80$.

$$
\begin{aligned}
m(T;\sigma_b) &= \int_0^\infty Th(T;\sigma_b)dT \\
&= \int_0^\infty m(T)h(d;\sigma_b)d\,d \\
&\approx 2\int_{d_L}^\infty \frac{L}{2kd}\frac{1}{\sqrt{2\pi}\sigma_d}\exp[-d^2/(2\sigma_d^2)]d\,d \\
&\approx \frac{cL^{5/2}}{4\sqrt{2\pi}k\sigma_b}. \qquad (30)
\end{aligned}
$$

The mean duration thus increases in proportion to the five-halves power of the number L of neurons. Figure 12 shows the ensemble mean $m(T;\sigma_b)$ of the duration in the networks with $\sigma_b=0.01$ against $L^{5/2}$ $(10\leq L\leq 100)$. Plotted is the mean duration of 10 000 oscillations obtained with computer simulation of Eq. (1) (solid circles), in which $x_{b(n)}$ and $x_n(0)$ are given as above. Plotted also are the estimates with the numerical integral with Eqs. (25) and (28) (a solid line), and Eq. (30) multiplied by 0.2 (a dashed line). Estimation with the simulation is unstable for large L since the SD of the duration for $L\geq 50$ was about ten times as large as the mean owing to the power-law tail of the distribution. The simulation results fit about to the estimates with the numerical integral, but tend to be lower than them for $L\geq 80$. The large value at $L=85$ is due to one outlier. This decrease for large L is also ascribed to the nonuniformity in the distribution of the initial block length l_0 due to the generation of four or more blocks, as mentioned in the last part of Sec. IV B. The exponent of the power of L in the estimates with the numerical integral is slightly larger than 5/2 and is close to 3. Equation (30) is about five times as large as the simulation results and the estimates with the numerical integral, which is due to the fact that the approximation of the probability density function by Eq. (29) agrees with Eq. (28) only for large T. Although there is such inconsistency, the increasing rate of the mean duration become more than five-halves power of the number L of neurons owing to the power-law distribution of the duration due to variations in the mean bias.

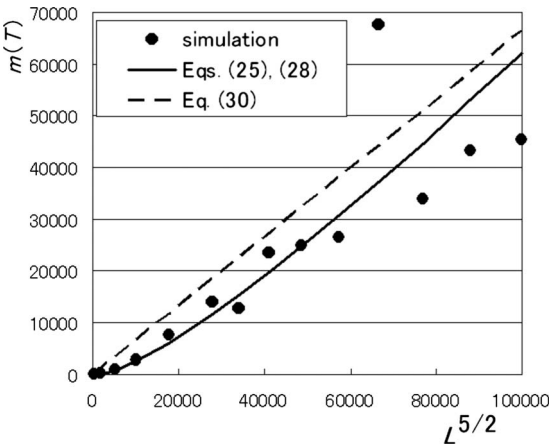

FIG. 12. Ensemble mean $m(T;\sigma_b)$ of the duration in the networks with $\sigma_b=0.01$ against $L^{5/2}$ $(10\leq L\leq 100)$. Plotted are the mean duration of 10 000 oscillations obtained with computer simulation of Eq. (1) (solid circles), the estimates with the numerical integral with Eqs. (25) and (28) (a solid line), and Eq. (30) multiplied by 0.2 (a dashed line).

V. CONCLUSION AND FUTURE WORK

The kinematical description of the traveling waves in the ring networks of unidirectionally coupled neurons in the presence of additive noise and spatial variations was derived. When the couplings are positive or in general the number of negative couplings is even, generated are at lease two traveling waves of the boundaries of the blocks of the neurons in which the signs of the states are the same and thus there are inconsistencies at the boundaries. These traveling waves result in the oscillations of the states of the neurons. The velocities of the two boundaries depend on the difference of the exponential of the lengths of the blocks (the numbers of neurons in the blocks) and their difference becomes exponentially small as the number of neurons increases. As a result it takes an exponentially long time until the two boundaries collide and the blocks merge so that the oscillation ceases.

First, it was shown that additive noise of intermediate strength extends the duration of the transient oscillations when the initial states of the neurons are fixed, e.g., the ini-

tial lengths of the blocks of the neurons are fixed. The exponential nonlinearity in the interaction between the traveling waves causes these noise-sustained oscillations. Further, the duration of the noise-sustained oscillations is distributed approximately in a power-law form of exponent 2. When increasing the number of neurons with the smaller initial block length fixed, the mean duration of the oscillations increases with the larger initial block length. These behaviors resemble those of the FPT of the Wiener process. The exponential increases in the duration with the number of neurons still remain although the mean duration of the oscillations occurring under random initial conditions decreases as the noise strength increases.

Next, it was shown that random biases or shifts in the steady states reduce the increasing rate of the duration of the transient oscillations with the number of neurons from an exponential order to polynomial. These spatial variations cause nonzero difference between the velocities of the traveling waves of the boundaries of the blocks of the neurons. The duration of the oscillations then increases almost linearly with the initial block length. Consequently, the duration of the oscillations occurring under random initial conditions is then distributed uniformly in most regions as the absolute values of the mean of biases or shifts increase. The mean duration then increases in proportion only to the number of neurons under fixed configurations of biases or shifts. Further, the distribution of the duration of the oscillations in an ensemble of the networks with random biases obeying an identical distribution has a power-law form of exponent 2 below the cutoff. The ensemble mean of the duration then increases in proportion about to the five-halves power of the number of neurons. This reduction of the increasing rates of the duration of the oscillations is caused by the asymmetry of the output function and the exponential increases remain when the mean bias is not shifted even though the value of each bias varies.

The exponential dependence of the transient time on the system size has also been found in more complicated patterns and systems as mentioned in Sec. I. It is expected that transient spatiotemporal chaos in complex systems, e.g., coupled map lattices is caused by intrinsically similar mechanism to that in the ring neural networks. Spatiotemporal noise and spatial variations can then have qualitatively the same effects on the transient time in these systems as that obtained in this paper. In particular, resonancelike effects with spatiotemporal noise might exist and enhance chaotic dynamics in the transient states. Effects of noise and variations on the transient chaos in these systems are of interest and their analysis is future work.

APPENDIX: PROPERTIES OF THE DURATION OF THE OSCILLATIONS WITHOUT NOISE AND BIASES

Properties of the duration of the transient oscillations in the following ring neural network in the absence of noise and biases are summarized [12]:

$$\tau dx_1/dt = -x_1 + f(x_L),$$

$$\tau dx_n/dt = -x_n + f(x_{n-1}), \quad (2 \le n \le L),$$

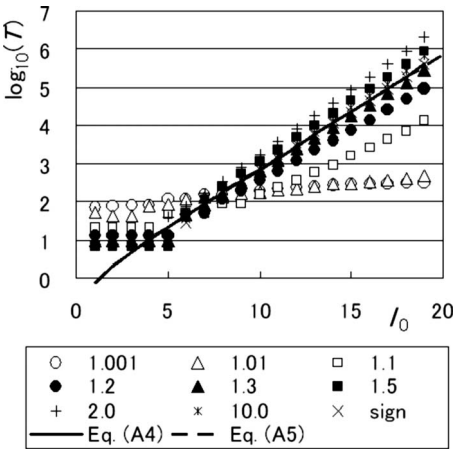

FIG. 13. Semilog plot of the duration T vs the initial block length l_0 $(1 \le l_0 \le 19)$ in the network of 40 neurons $(L=40)$ without noise and biases. Plotted are the results of computer simulation of Eq. (A1) under Eq. (14) with several values of g (symbols), Eq. (A4) (a solid line), and Eq. (A5) (a dashed line).

$$f(x) = \tanh(gx), \quad (g > 1). \tag{A1}$$

As shown in Fig. 1(a), the neurons are soon divided in two blocks in which the signs of the states x_n of neurons are the same and the boundaries between the blocks travel in the direction of the coupling. The length l of the smaller block (the number of neurons in the block) changes as

$$\begin{aligned} dl/dt &= 1/\{\tau[\ln 2 + \ln(1 - 2^{-(L-l)})]\} \\ &\quad - 1/\{\tau[\ln 2 + \ln(1 - 2^{-l})]\} \\ &\approx k\{\exp[-c(L-l)] - \exp(-cl)\}, \end{aligned}$$

$$k = 1/[\tau(\ln 2)^2], \quad c = \ln 2 \tag{A2}$$

and the solution is given by

$$\begin{aligned} \exp[cl(t)] &= \exp(cL/2)\tanh(-\exp(-cL/2)ckt \\ &\quad + \operatorname{arctanh}\{\exp[c(l_0 - L/2)]\}), \end{aligned}$$

$$l_0 = l(0), \quad (0 \le l_0 \le L/2). \tag{A3}$$

The duration T of the transient oscillations is given by setting $l(T)=0$,

$$\begin{aligned} T &= 1/(ck)\exp(cL/2)(\operatorname{arctanh}\{\exp[c(l_0 - L/2)]\} \\ &\quad - \operatorname{arctanh}[\exp(-cL/2)]). \end{aligned} \tag{A4}$$

A simpler form is obtained by letting L be infinity as

$$dl/dt = -k\exp(-cl),$$

$$l(t) = 1/c\ \ln[\exp(cl_0) - ckt],$$

$$T = [\exp(cl_0) - 1]/(ck), \quad [l(T) = 0]. \tag{A5}$$

These expressions are applicable to the networks with not so small coupling gains [10]. Figure 13 shows a semilog plot of the duration T against the initial block length l_0 $(1 \le l_0 \le 19)$ in the network of 40 neurons $(L=40)$. Plotted are the

results of computer simulation of Eq. (A1) under the initial condition Eq. (14) (symbols), Eq. (A4) (a solid line), and Eq. (A5) (a dashed line). Computer simulation was done using the simple Euler method with a time step 0.01. The results for the coupling gain $g=1.001$ (open circles), 1.01 (open triangles), 1.1 (open squares), 1.2 (solid circles), 1.3 (solid triangles), 1.5 (solid squares), 2.0 (daggers), and 10.0 (asterisks) are plotted. The result of computer simulation with the sign function [Eq. (2)] and a time step 10^{-6} was also plotted (crosses). The duration increases exponentially with the initial block length (the number of neurons in the initial smaller block). Equations (A4) and (A5) hardly differ from each other and agree with the simulation results for $g \geq 1.2$, while the increasing rates vary slightly. The increasing rates reduce as the coupling gain decreases to unity ($g \leq 1.1$), in which the stable states of the neurons are close to zero ($\pm x_p \approx 0$) and the kinematics with the sign function ($x_p=1$) is inappropriate.

When the initial states $x_n(0)$ of neurons are given randomly, the initial length l_0 of the generated smaller block is distributed uniformly in $(0, L/2)$. The probability density function h of the duration of the transient oscillations is then obtained as

$$\begin{aligned} h(T) &= |dT(l_0;L)/dl_0|^{-1}/(L/2) \\ &= 2k \exp(-cL/2)\mathrm{cosech}(2\{\exp(-cL/2)ckT \\ &\quad + \mathrm{arctanh}[\exp(-cL/2)]\})2/L. \end{aligned} \tag{A6}$$

There is a cutoff point $T_c=\exp(cL/2)/(ck)$ at which the form of the probability density function changes. When $T<T_c$, the approximate form is derived by using $\mathrm{arctanh}(\varepsilon) \approx \varepsilon$ and $\sinh(\varepsilon) \approx \varepsilon$ as

$$\begin{aligned} h(T) &\approx k/(ckT+1)2/L, \quad \{0 \leq T \leq T_c = [\exp(cL/2) \\ &\quad - 1]/(ck)\}, \end{aligned} \tag{A7}$$

which is also derived directly from Eq. (A5). The duration T is thus distributed in the form of $1/T$. When $T>T_c$, the form is approximated by the exponential distribution by using $\sinh(x) \approx \exp(x)/2$ $(x \gg 1)$ for large T as

$$h(T) \approx \lambda \exp(-\lambda T), \quad \lambda \approx 2ck \exp(-cL/2), \quad (T \geq T_c). \tag{A8}$$

The mean m, the variance σ^2, and the coefficient of variation C_V of the duration T are expressed by using Eqs. (A5) and (A7) for large L as

$$\begin{aligned} m[T(L)] &= 2[\exp(cL/2) - 1 - cL/2]/(c^2kL), \\ \sigma^2(T(L)) &= [\exp(cL) - 4\exp(cL/2) + 3 + cL]/(c^3k^2L) \\ &\quad - \{m[T(L)]\}^2, \\ C_V[T(L)] &= \sigma[T(L)]/m[T(L)] \approx (cL)^{1/2}/2, \quad (L \gg 1). \end{aligned} \tag{A9}$$

The mean and standard deviation increase exponentially with the number L of neurons.

[1] Y. Kuramoto, *Chemical Oscillations, Waves, and Turbulence* (Springer, New York, 1984); M. Markus and V. P. Munuzuri, *Discretely Coupled Dynamical Systems* (World Scientific, Singapore, 1997); *Pattern Formation in Continuous and Coupled Systems*, edited by M. Golubitsky *et al.* (Springer, New York, 1999).

[2] S. Amari, *Mathematics of Neural Networks* (Sangyo-Tosho, Tokyo, 1978); M. W. Hirsh, Neural Netw. **2**, 331 (1989).

[3] A. F. Atiya and P. Baldi, Int. J. Neural Syst. **1**, 103 (1989).

[4] T. Gedeon, *Cyclic Feedback Systems, Memoirs of the American Mathematical Society* (American Mathematical Society, Providence, 1998).

[5] F. Pasemann, Neural Netw. **8**, 421 (1995).

[6] S. Guo and L. Huang, Acta Math. Sin. **23**, 799 (2007); X. Xu, J. Phys. A **41**, 035102 (2008).

[7] P. Baldi and A. F. Atiya, IEEE Trans. Neural Netw. **5**, 612 (1994); K. Pakdaman *et al.*, Phys. Rev. E **55**, 3234 (1997).

[8] K. L. Babcock and R. M. Westervelt, Physica D **23**, 464 (1986); **28**, 305 (1987).

[9] H. Kitajima and Y. Horikawa, in Proceedings of the 2007 International Symposium on Nonlinear Theory and its Applications, edited by L. Trajkovic and K. Okumura (IEICE, Japan, 2007), p. 453.

[10] H. Kitajima and Y. Horikawa, Chaos, Solitons Fractals **42**, 1854 (2009).

[11] Y. Horikawa and H. Kitajima, in *Noise and Fluctuations*, edited by M. Tacano *et al.*, AIP Conf. Proc. No. 922 (AIP, Melville, NY, 2007), p. 569.

[12] Y. Horikawa and H. Kitajima, Physica D **238**, 216 (2009).

[13] K. Kawasaki and T. Ohta, Physica A **116**, 573 (1982); J. Carr and R. L. Pego, Commun. Pure Appl. Math. **42**, 523 (1989); S. Ei and T. Ohta, Phys. Rev. E **50**, 4672 (1994).

[14] Y. Horikawa, Phys. Rev. E **78**, 066108 (2008).

[15] M. C. Cross and P. C. Hohenberg, Rev. Mod. Phys. **65**, 851 (1993).

[16] M. J. Ward, SIAM J. Appl. Math. **56**, 1247 (1996); in *Boundaries, Interfaces, and Transitions*, CRM Proceedings and Lecture Notes, edited by M. C. Delfour (American Mathematical Society, Providence, 1998), Vol. 13, p. 237; references therein.

[17] K. Kaneko, Phys. Lett. A **149**, 105 (1990); A. Wacker, S. Bose, and E. Schöll, Europhys. Lett. **31**, 257 (1995); R. Zillmer *et al.*, Neurocomputing **70**, 1960 (2007).

[18] U. Bastolla and G. Parisi, J. Phys. A **31**, 4583 (1998); J. Šíma and P. Orponen, Theor. Comput. Sci. **306**, 353 (2003).

[19] J. Rinzel, in *Dynamics and Modeling of Reactive Systems*, edited by W. E. Stewart *et al.* (Academic, New York, 1980), p. 259; J. Rinzel and K. Maginu, in *Nonequilibrium Dynamics in Chemical Systems*, edited by C. Vidal and A. Pacault (Springer, New York, 1984), p. 107.

[20] G. B. Whitham, *Linear and Nonlinear Waves* (John Wiley & Sons, New York, 1974); R. Haberman, *Mathematical Model: Traffic Flow* (Prentice-Hall, Englewood Cliffs, NJ, 1977).

[21] G. Orosz, B. Krauskopf, and R. E. Wilson, Physica D **211**, 277 (2005).
[22] G. Gutierrez, in *Wiley Encyclopedia of Electrical and Electronics Engineering 23*, edited by G. Webster (John Wiley & Sons, New York, 1999), p. 75.
[23] Y. Horikawa and H. Kitajima (unpublished).
[24] W. Horsthemke and R. Lefever, *Noise-Induced Transitions* (Springer, New York, 1984); L. Gammaitoni *et al.*, Rev. Mod. Phys. **70**, 223 (1998); P. S. Landa and P. V. E. McClintock, Phys. Rep. **323**, 1 (2000); B. Lindner *et al.*, *ibid.* **392**, 321 (2004).
[25] F. Schlögl, C. Escher, and R. S. Berry, Phys. Rev. A **27**, 2698 (1983); A. Vl. Gurevich, S. L. Leikin, and R. G. Mints, Phys. Lett. **105**, 31 (1984); A. Engel, *ibid.* **113**, 139 (1985).
[26] Y. Horikawa, in Proceedings of the 2008 International Symposium on Nonlinear Theory and its Applications, edited by G. Kolumban and T. Endo (IEICE, Japan, 2008), p. 524.
[27] Y. Horikawa and H. Kitajima, Neurocomputing (to be published).
[28] N. S. Goel and N. Richter-Dyn, *Stochastic Models in Biology* (Academic Press, New York, 1974).
[29] W. Feller, *An Introduction to Probability Theory and Its Applications 2*, 2nd ed. (John Wiley & Sons, New York, 1966).